

Supporting Information

Contents

	page
1. Sample preparation	2
2. Photoexcitation spectrum of Tb ion	3
3. Details of PL lifetime calculations	4
4. SDF for transient Tb states	6
5. Steady state PL data	7

1. Sample preparation

The DOC/SWNT/Tb hydrogel samples were prepared by using two methods: terbium chloride solution was incorporated in the hydrogel during the synthesis; alternatively it was dropped into the NMR tube with (already synthesized) hydrogel before the experiment. After several days both types of Tb/DOC/SWNT hydrogel samples showed similar properties, although, PL lifetime was found to be slightly shorter (2.1 ms compared to 2.3ms) for the latter method (a typical sample is shown on Fig. S1).

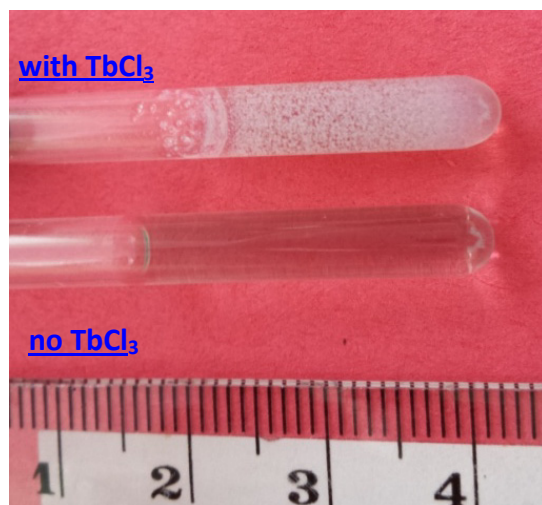


Figure S1.DOC/SWNT hydrogel sample: (bottom) original sample; (top) similar sample after several days upon adding terbium chloride.

2. Photoexcitation spectrum of Tb ion.

PLE of terbium is asymmetric, showing a narrow peak with the maximum at 488nm shifted toward the shorter wavelength and a line width of 4 nm. This allowed us to apply laser line at $\lambda = 486$ nm for excitation and use 488 nm long pass filter to cut off the scattered and/or incident laser beam.

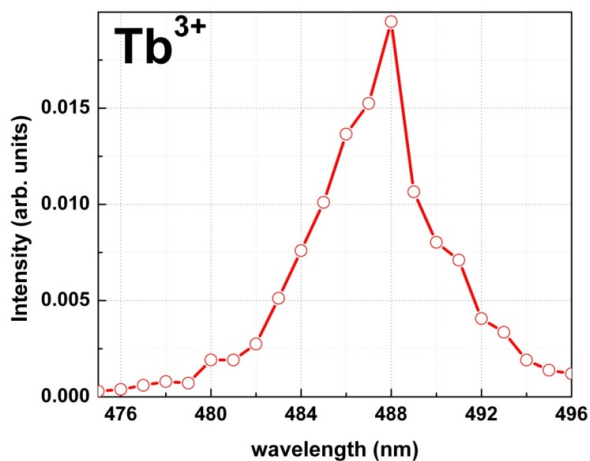


Figure S2. PL intensity for the peak at 545 nm vs. excitation wavelength in TbCl₃ DI water solution.

3. Details of PL lifetime calculations.

For Figure 2d the PL curves at different times of diffusion were fitted by bi-exponential fit. In Figure S3 we present the original data, the fit and the residuals. Similar fit was done for Tb PL in DOC water solutions. A sample fit/data/residuals are presented in Figure S4.

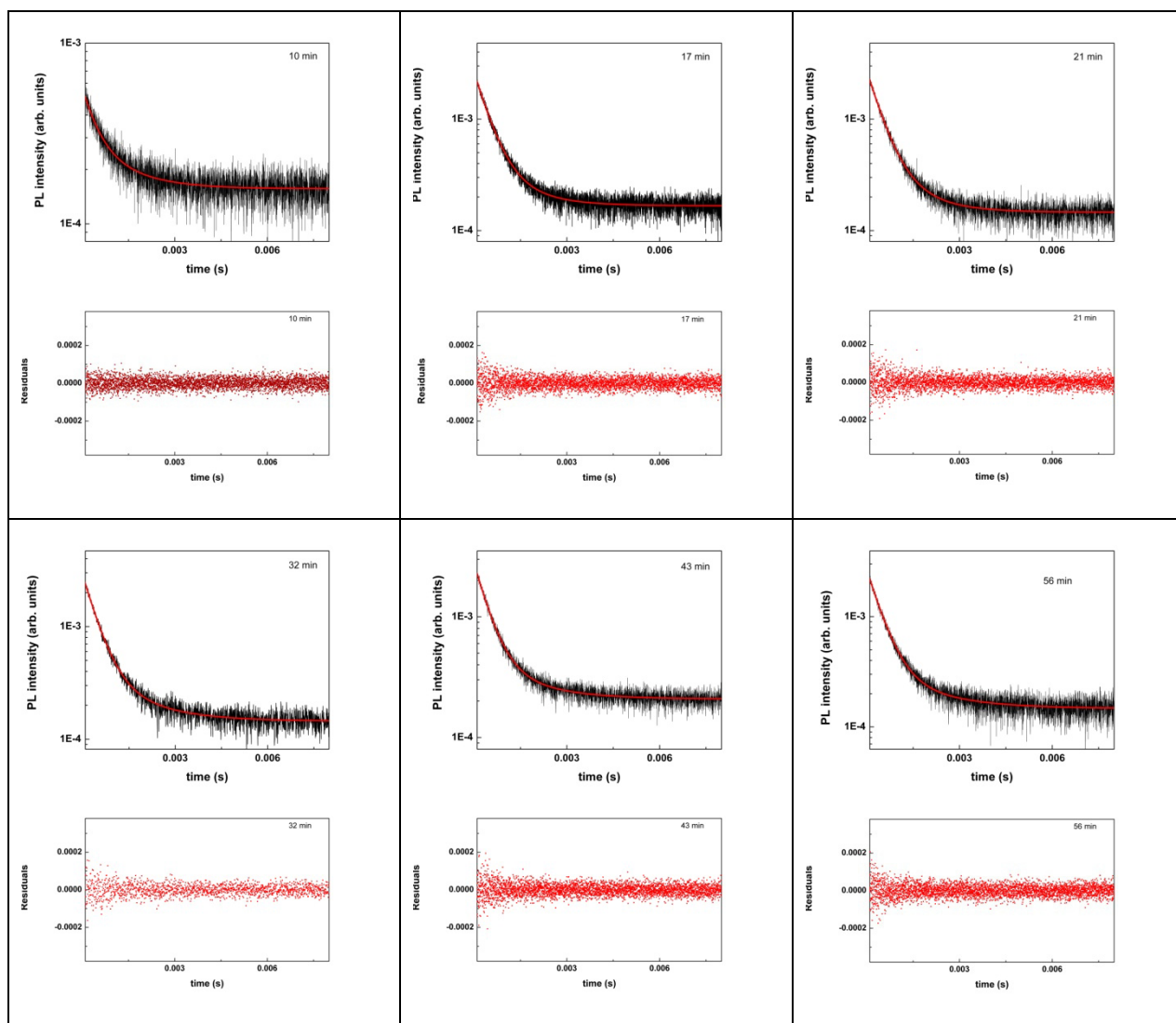


Figure S3. The PL decay of Tb^{3+} in DOC/SWNT hydrogel with time. Excitation wavelength is 486 nm, emission wavelength is 545 nm. Top panels show bi-exponential fit, bottom panels show residuals.

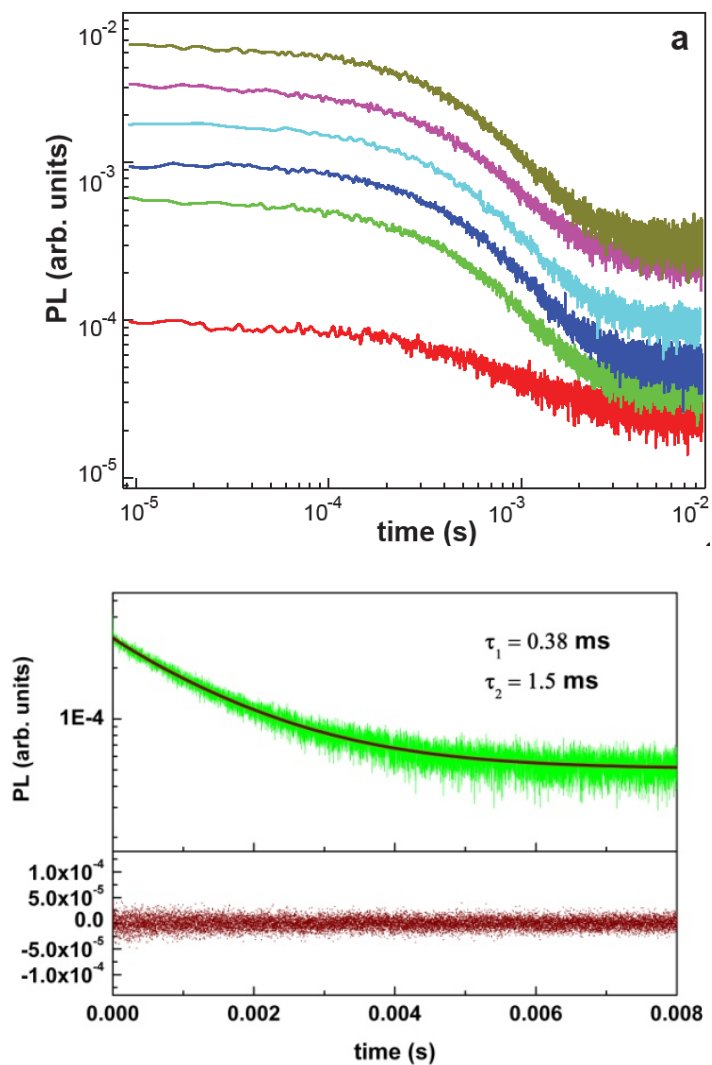


Figure S4. (top) Same data as in figure 2a of main text, presented in double-log scale, instead. (bottom) PL decay curve of Tb/DOC water solution with bi-exponential fit (overlaid) and residuals.

4. SDF for transient Tb states.

Stretched exponential¹ dependence of the Tb PL decay, presented in Figure 3a, allows analysis via SDFs. Figure S5 shows change of characteristic lifetimes of transient Tb complexes versus diffusion depth.

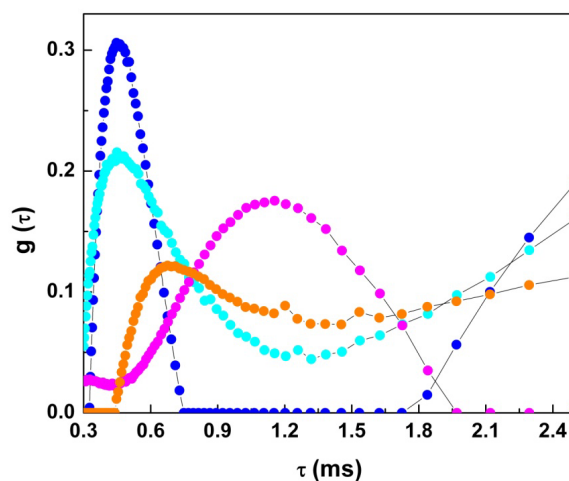


Figure S5. Spectral distribution function calculated for Tb-complexes upon diffusion into silica hydrogel taken 80 min after adding Tb on the top of the sample at 4 loci as in Fig. 3.

¹ De Michele, C.; Del Gado, E.; Leporini, D., Scaling between structural relaxation and particle caging in a model colloidal gel. *Soft Matter* 2011, 7 (8), 4025-4031.

Ganazzoli, F.; Raffaini, G.; Arrighi, V., The stretched-exponential approximation to the dynamic structure factor in non-entangled polymer melts. *Physical Chemistry Chemical Physics* 2002, 4 (15), 3734-3742.

Hakansson, P.; Westlund, P. O.; Lindahl, E.; Edholm, O., A direct simulation of EPR slow-motion spectra of spin labelled phospholipids in liquid crystalline bilayers based on a molecular dynamics simulation of the lipid dynamics. *Physical Chemistry Chemical Physics* 2001, 3 (23), 5311-5319.

Ko, H.-C.; Yuan, C.-T.; Tang, J., Probing and controlling fluorescence blinking of single semiconductor nanoparticles. *Nano Reviews; Vol 2 (2011) incl Supplements* 2011.

Langer, J. S., Shear-transformation-zone theory of viscosity, diffusion, and stretched exponential relaxation in amorphous solids. *Physical Review E* 2012, 85 (5), 051507.

Ruiz-García, M.; Prados, A., Kovacs effect in the one-dimensional Ising model: A linear response analysis. *Physical Review E* 2014, 89 (1), 012140.

Somoza, M. M.; Sluch, M. I.; Berg, M. A., Torsional Relaxation and Friction on the Nanometer Length Scale: Comparison of Small-Molecule Rotation in Poly(dimethylsiloxane) and Poly(isobutylene). *Macromolecules* 2003, 36 (8), 2721-2732.

5. Steady state PL data.

We observed substantial differences in the peak shape of the steady state PL of Tb in different environments. In Figure 1a (inset) the PL in both DOC/SWNT hydrogel (red) and the water solution containing no surfactant (blue) are shown. The changes in the shape of the peaks are likely due to the “crystal” field of the environment. One could attribute a less structured shape of these peaks to the weaker interaction with the water environment when the Tb is inside the micelles. Figure S7 shows evolution of PL peaks ${}^5D_4 \rightarrow {}^7F_j$, $j=4-7$ (labeled in Figure S6a, inset), during the DOC complex formation in $TbCl_3$ water solution. PL intensity increases upon increasing concentration of the DOC in water solution (black to purple).

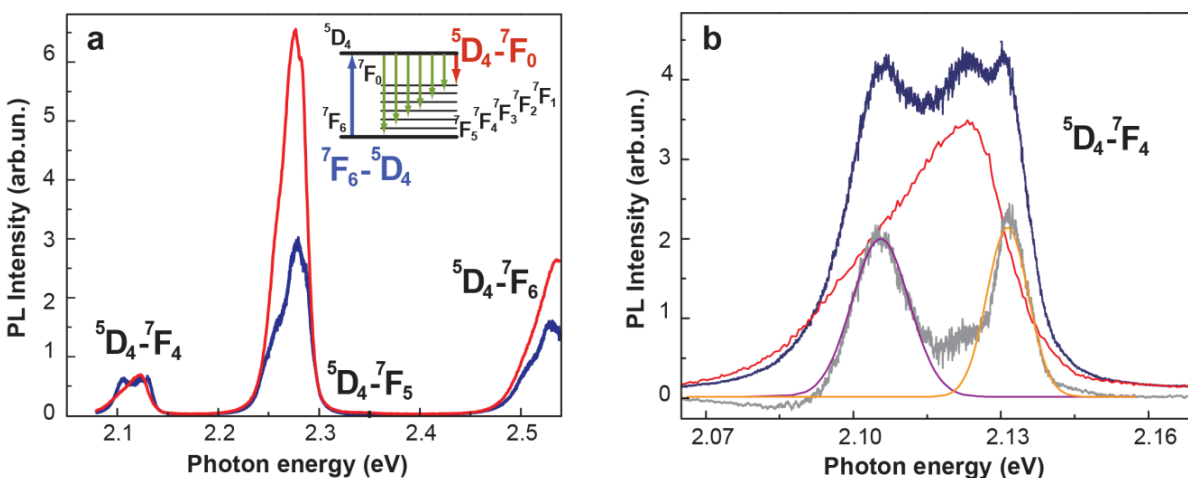


Figure S6. (a) PL spectra of Tb in DOC/SWNT hydrogel (red), water solution (blue), DOC water solution (green). PL of ${}^5D_4 \rightarrow {}^7F_5$ and ${}^5D_4 \rightarrow {}^7F_4$ transitions under 488 nm of excitation is measured. (b) Line shape of ${}^5D_4 \rightarrow {}^7F_4$ peak in water (blue), DOC/SWNT hydrogel (red) and their difference (black), fitted with 2 Gaussian peaks.

We study the peak structure of ${}^5D_4 \rightarrow {}^7F_4$ transition line in details. Figure S6b shows this transition for free (solvated) Tb ion (blue) and for Tb inside the DOC micelles confined in the pores of the hydrogel (red). The curve difference (grey) is well fitted by two Gaussian peaks. These peaks could be due to vibronic satellites of one of the optical transitions since they have the energy compatible with several Raman lines of O-H vibrations [P. K. Narayanaswamy, Proc.

Indian Acad. Sci., 1948, 27, 311-315.] (note that those can slightly shift in hydration water shell). This is a subject of separate forthcoming study.

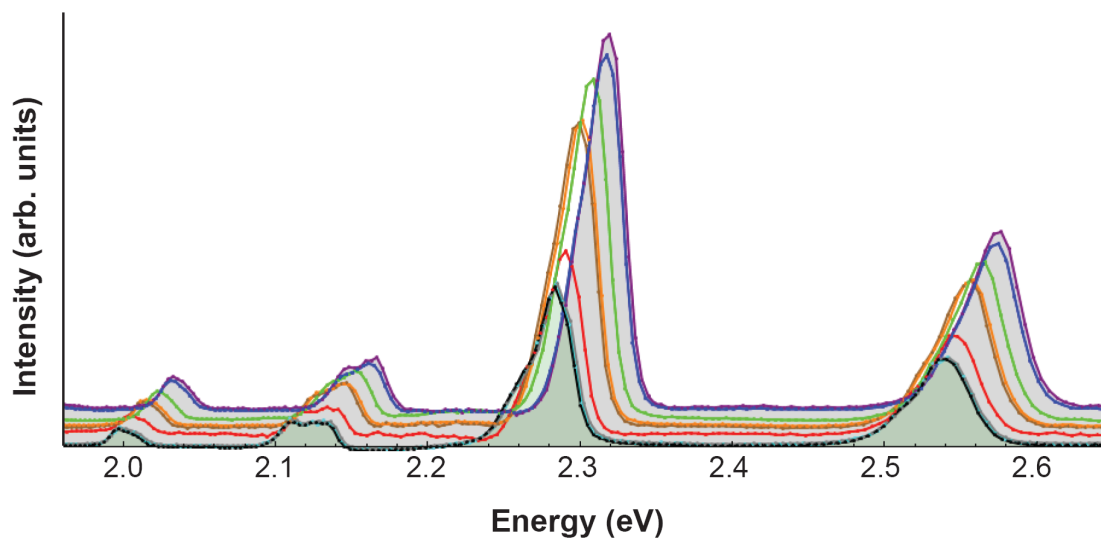


Figure S7. Steady-state PL spectra for Tb-complexes in solution with increasing DOC concentration (black-to-purple) under 360 nm of excitation.

Close similarity of the spectra of Tb in DOC micelles (in bulk water) and inside the hydrogel confirms that the DOC gelation and following Tb encapsulation in the DOC micelles are intermediate steps for formation of the long-lived complexes in ordered DOC phase in both systems.

Figure S8 shows partial quantum yield (QY) for four lowest optical transitions, estimated via the integral under the PL peaks (data points) and evaluated using Eq. (3) of main text.

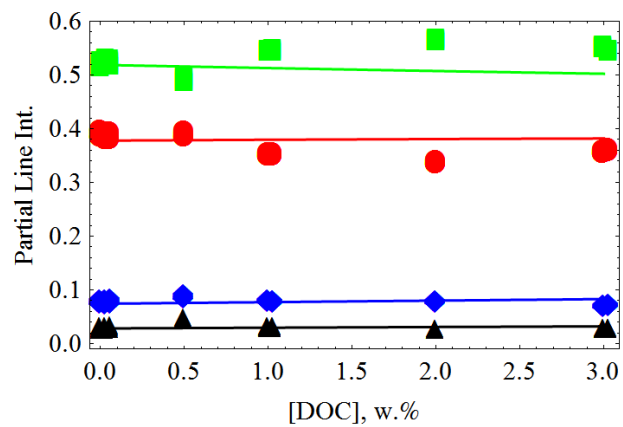


Figure S8. Partial QY as a function of DOC concentration: [NaDOC] = 0,12, 24.2, 48.9 and 74.1 mM in 0.3M TbCl₃ water solution.